



---

**Título artículo / Títol article:**

**Effects of green space spatial pattern on land surface temperature: Implications for sustainable urban planning and climate change adaptation**

**Autores / Autors**

**Maimaitiyiming, Matthew ; Ghulam, Abduwasit ; Tiyip, Tashpolat ; Pla Bañón, Filiberto ; Latorre Carmona, Pedro ; Halik, Ümüt ; Sawu, Mamat ; Caetano, Mario**

**Revista:**

**ISPRS Journal of Photogrammetry and Remote Sensing**

**Versión / Versió:**

**Postprint**

**Cita bibliográfica / Cita bibliogràfica (ISO 690):**

**MAIMAITIYIMING, Matthew, et al. Effects of green space spatial pattern on land surface temperature: Implications for sustainable urban planning and climate change adaptation. ISPRS Journal of Photogrammetry and Remote Sensing, 2014, vol. 89, p. 59-66.**

**url Repositori UJI:**

**<http://hdl.handle.net/10234/135506>**

---

1  
2  
3  
4 1 **Effects of green space spatial pattern on land surface temperature:**

5  
6  
7 2 **implications for sustainable urban planning and climate change adaptation**

8  
9  
10 3  
11  
12 4 Matthew Maimaitiyiming<sup>a</sup>, Abduwasit Ghulam<sup>a</sup>, Tashpolat Teyip<sup>b,c</sup>, Filiberto Pla<sup>d</sup>, Pedro

13  
14  
15 5 Latorre-Carmona<sup>d</sup>, Mário Caetano<sup>e</sup>, Mamat Sawut<sup>a,b,c</sup>, Ümüt Halik<sup>b,c</sup>

16  
17 6  
18  
19  
20 7 <sup>a</sup> Center for sustainability, Saint Louis University, Saint Louis, MO 63103, USA

21  
22 8  
23  
24 9 <sup>b</sup> College of Resources and Environmental Sciences, Xinjiang University, Urumqi, Xinjiang  
25  
26  
27 10 830046, China

28  
29  
30 11  
31  
32 12 <sup>c</sup> Ministry of Education Key Laboratory of Oasis Ecology at Xinjiang University, Urumqi,  
33  
34 13 Xinjiang 830046, China

35  
36  
37 14  
38  
39 15 <sup>d</sup> Institute of New Imaging Technologies, University Jaume I, 12071 Castellón, Spain

40  
41 16  
42  
43  
44 17 <sup>e</sup> Institute for Statistics and Information Management (ISEGI), Universidade Nova de Lisboa,  
45  
46 18 Campus de Campolide, 1070-312, Lisboa, Portugal

47  
48  
49 19  
50  
51  
52 20  
53  
54 21 **Abstract**—The urban heat island (UHI) refers to the phenomenon of higher atmospheric  
55  
56 22 and surface temperatures occurring in urban areas than in the surrounding rural areas. Mitigation  
57  
58  
59 23 of the UHI effects via the configuration of green spaces and sustainable design of urban  
60  
61

1  
2  
3  
4  
5  
6  
7  
8  
9  
10  
11  
12  
13  
14  
15  
16  
17  
18  
19  
20  
21  
22  
23  
24  
25  
26  
27  
28  
29  
30  
31  
32  
33  
34  
35  
36  
37  
38  
39  
40  
41  
42  
43  
44  
45  
46  
47  
48  
49  
50  
51  
52  
53  
54  
55  
56  
57  
58  
59  
60  
61  
62  
63  
64  
65

24 environments has become an issue of increasing concern under changing climate. In this paper,  
25 the effects of the composition and configuration of green space on land surface temperatures  
26 (LST) were explored using landscape metrics including percentage of landscape (PLAND), edge  
27 density (ED) and patch density (PD). An oasis city of Aksu in Northwestern China was used as a  
28 case study. The metrics were calculated by moving window method based on a green space map  
29 derived from Landsat Thematic Mapper (TM) imagery, and LST data were retrieved from  
30 Landsat TM thermal band. Normalized mutual information measure was employed to investigate  
31 the relationship between LST and the spatial pattern of green space. The results showed that  
32 while the PLAND is the most important variable that elicits LST dynamics, spatial configuration  
33 of green space also has significant effect on LST. Though, the highest normalized mutual  
34 information measure was with the PLAND (0.71), it was found that ED and PD combination is  
35 the most deterministic factors of LST than the unique effects of a single variable or the joint  
36 effects of PLAND and PD or PLAND and ED. Normalized mutual information measure  
37 estimations between LST and PLAND and ED, PLAND and PD and ED and PD were 0.7679,  
38 0.7650 and 0.7832, respectively. A combination of the three factors PLAND, PD and ED  
39 explained much of the variance of LST with a normalized mutual information measure of  
40 0.8694. Results from this study can expand our understanding of the relationship between LST  
41 and street trees and vegetation, and provide insights for sustainable urban planning and  
42 management under changing climate.

43  
44  
45 **Keywords**—urban heat island, urban green space, landscape metrics, configuration, normalized  
46 mutual information measure.

## 1. Introduction

The urban heat island (UHI) refers to the phenomenon of higher atmospheric and surface temperatures occurring in urban areas than in the surrounding rural areas. This phenomenon is widely observed in cities regardless of their sizes and locations (Connors et al., 2013; Cui and de Foy, 2012; Imhoff et al., 2010; Li et al., 2012; Tran et al., 2006). The UHI is mainly caused by the modification of land surfaces by urban development, which uses materials that effectively store short-wave radiation (Solecki et al., 2005). As the result, land surface temperature (LST) increases due to the UHI, which may disrupt species composition and distribution (Niemelä, 1999) by increasing the length of growing seasons, decrease air quality (Feizizadeh and Blaschke, 2013; Lai and Cheng, 2009; Sarrat et al., 2006; Weng and Yang, 2006), leading to greater health risks (Patz et al., 2005). The UHI may also decrease water quality as warmer waters flow into streams putting additional stress on aquatic ecosystems (James, 2002). Therefore, it has become a major research focus in urban climatology and urban ecology since first reported in 1818 (Howard, 1818).

The intensity and spatial pattern of UHI are largely exacerbated from population dynamics and development of build-up areas (Arnfield, 2003; Wu et al., 2013). Specifically, urban structure (e.g. height-to-width ratio of buildings and streets), , proportion of built-up versus green spaces per unit area, weather conditions (e.g. wind and humidity), and socioeconomic activities determine the development of the UHI (Hamdi and Schayes, 2007; Rizwan et al., 2008b; Taha, 1997; Unger, 2004; Voogt and Oke, 1998). For example, Huang et al. (2011) found statistically significant relationship between the UHI and socioeconomic factors indicating that a higher UHI effects were linked to block groups characterized by low income, high poverty, less education, more ethnic minorities, more elderly people and greater risk of

1  
2  
3  
4 70 crime. As many of these factors, especially land surface characteristics are primarily represented  
5  
6  
7 71 by land-cover and land-use (LCLU), the relationship between the LST and LCLU has been the  
8  
9 72 focus of numerous studies on the UHI (Buyantuyev and Wu, 2010; Dousset and Gourmelon,  
10  
11 73 2003; Pu et al., 2006; Voogt and Oke, 2003;Weng et al., 2004). This is due to the fact that  
12  
13  
14 74 vegetation usually has higher evapotranspiration and lower emissivity than built-up areas, and  
15  
16 75 thus has lower surface temperatures (Hamada and Ohta, 2010; Weng et al., 2004).

17  
18  
19 76         Composition and configuration of green spaces are the two major elements of LCLU. The  
20  
21 77 former refers to the abundance and variety of land cover types and the latter is related to the  
22  
23 78 spatial arrangements and layout of land cover types (Connors et al., 2013; Turner, 2005).  
24  
25  
26 79 Remarkable proliferations of studies focusing on the relationship between LST and green space  
27  
28 80 composition has been reported over the last two decades (Chen et al., 2006; Tran et al., 2006;  
29  
30  
31 81 Voogt and Oke, 2003; Weng, 2009; Weng et al., 2004). Though the magnitude of correlations  
32  
33 82 varied among these reports, a negative relationship between the vegetation amount/fraction and  
34  
35  
36 83 LST was consistently observed. However, the spatial characteristics and configurations of  
37  
38 84 vegetation patches within the urban environment have significant impacts on the distribution of  
39  
40  
41 85 the UHI (Bowler et al., 2010; Cao et al., 2010; Honjo and Takakura, 1991; Yokohari et al., 1997;  
42  
43 86 Zhao et al., 2011), and that the size and shape of a vegetation patch creates cool island effects, a  
44  
45  
46 87 phenomenon that the temperature of green space is lower than its surrounding areas (Cao et al.,  
47  
48 88 2010; Zhang et al., 2009). Based on a case study of a heavily urbanized Beijing metropolitan  
49  
50  
51 89 area in China, Li et al. (2012) also indicated that increasing patch density results in significantly  
52  
53 90 higher LST when the size of urban green space unaffected, and that spatial configuration has a  
54  
55 91 significant influence in the variability of derived LST.

1  
2  
3  
4  
5  
6  
7  
8  
9  
10  
11  
12  
13  
14  
15  
16  
17  
18  
19  
20  
21  
22  
23  
24  
25  
26  
27  
28  
29  
30  
31  
32  
33  
34  
35  
36  
37  
38  
39  
40  
41  
42  
43  
44  
45  
46  
47  
48  
49  
50  
51  
52  
53  
54  
55  
56  
57  
58  
59  
60  
61  
62  
63  
64  
65

92           It is evident from an exhaustive literature review hitherto that there is a lack of case  
93 studies within arid regions (Connors et al., 2013). As cities are growing fast in population, and  
94 urbanization is projected to be high (Baker et al. 2004), sustainable planning of urban  
95 environment to mitigate UHI effects highlights a pressing need for immediate attention. This is  
96 further emphasized by climate changes as arid regions are likely to become even drier in  
97 response to increasing temperature from global warming (Durack et al., 2012). Driven by fast  
98 economic growth and population increase, Northwestern China has experienced rapid  
99 urbanization in the past several decades, along with a drastic transformation of the urban  
100 environment and social equity (Fan and Qi, 2010; Halik et al., 2013; Liu et al., 2013). In  
101 addition, the majority of the previous studies used ordinary least squares regression and/or spatial  
102 autoregression to analyze the relationship between the landscape metrics and LST. The statistical  
103 significance of the relationship between the landscape metrics and LST varied between the  
104 methods (Li et al., 2012). Comparative approaches with additional case studies are needed to  
105 generalize the methods and concepts demonstrated by these preliminary attempts. To that end,  
106 we investigate the effects of composition and configuration of urban green space on LST using a  
107 robust moving window algorithm of normalized mutual information measure in the arid city of  
108 Aksu, Xinjiang Uyghur Autonomous Region in Northwestern China. One of the advantages of  
109 using mutual information measures is that it can capture linear as well as strongly non-linear  
110 relationships among variables under the “umbrella” of just one concept (“mutual information”).  
111 The goal is to provide guiding suggestions for sustainable urban planning and development  
112 under future climate changes. We chose to use Landsat 30 m resolution data as previous studies  
113 (Liu and Weng, 2009; Li et al., 2013) have demonstrated that 30 m and 90 m are the optimal

1  
2  
3  
4  
5  
6  
7  
8  
9  
10  
11  
12  
13  
14  
15  
16  
17  
18  
19  
20  
21  
22  
23  
24  
25  
26  
27  
28  
29  
30  
31  
32  
33  
34  
35  
36  
37  
38  
39  
40  
41  
42  
43  
44  
45  
46  
47  
48  
49  
50  
51  
52  
53  
54  
55  
56  
57  
58  
59  
60  
61  
62  
63  
64  
65

114 resolutions to study the relationship between LST and landscape patterns at patch level and  
115 landscape levels, respectively.

116 The paper is organized in the sections below. Following the description of the study area in  
117 Section 2, the methodology of calculating LST, landscape metrics, and a brief introduction to  
118 normalized mutual information measure are presented in Section 3. The results, discussions and  
119 conclusions are presented in Section 4, 5 and 6, respectively.

120

## 121 **2. Study area**

122

123 The study area, downtown Aksu City, Northwestern China, is a typical oasis city located in an  
124 arid region. Aksu City is the capital of Aksu Prefecture in Xinjiang Uyghur Autonomous Region,  
125 China. Geographically, the city is situated in south of the Tianshan Mountains and northwest  
126 edge of the Tarim Basin (39°30'N - 41°27'N, 79°39'E - 82°01'E; Fig. 1). Aksu City is known as  
127 “the Land of Melons and Fruits”. It includes municipal total area of 14,300 Km<sup>2</sup> and built-up area  
128 of 28.1 Km<sup>2</sup>.

129

130 Aksu City is rich in light and heat resources. It has a long frost-free period from 205 to 219 days.  
131 The climate is dry, and rainfall is extremely rare with less than 50 mm per year and average  
132 annual evaporation of 1950 mm. Topography of the study area is flat. The climatic and the  
133 physiographic conditions are mostly the same across the region. Therefore, it is an ideal area to  
134 explore the relationship between LST and spatial pattern of green space in arid and semi-arid  
135 land.

136

1  
2  
3  
4  
5  
6  
7  
8  
9  
10  
11  
12  
13  
14  
15  
16  
17  
18  
19  
20  
21  
22  
23  
24  
25  
26  
27  
28  
29  
30  
31  
32  
33  
34  
35  
36  
37  
38  
39  
40  
41  
42  
43  
44  
45  
46  
47  
48  
49  
50  
51  
52  
53  
54  
55  
56  
57  
58  
59  
60  
61  
62  
63  
64  
65

137 The proportion of green area in the metropolitan region has increased to 30.6% today from 12 %  
138 in early 1980s. Urban green space coverage has reached 39.2% with the per capita public green  
139 area of 9 m<sup>2</sup>. Meanwhile, city's ecological environment has been significantly improved. This  
140 rapid growth in green space emphasizes a need to develop most effective configuration of green  
141 space to reduce the urban heat island caused by expanding impervious surfaces and to adapt to  
142 the global climate change.

143  
144  
145 Insert Figure 1 here  
146

### 147 3. Methodology

#### 148 3.1. Land Surface Temperature

149 Landsat-5 Thematic Mapper (TM) thermal infrared band 6 (11.45 – 12.50μm) data with 120 ×  
150 120 m resolution were utilized to derive the LST (Fig. 2b). The satellite data were collected on  
151 August 19, 2011, which was a clear day with 0 % cloud cover. Meteorological variables that  
152 influence the intensity of urban heat environment at the time of image capture were obtained  
153 from China standard meteorological station in the study site. These variables include daily  
154 precipitation (0 mm), daily average wind speed (1.6 m/s), wind direction (South-East) and  
155 humidity (46 %). Due to the lack of detailed in-situ atmospheric variables that allow physical  
156 inversion of brightness temperature to LST, a mono-window algorithm was applied for retrieval  
157 of LST (Qin et al., 2001)

$$158 \quad T_s = [a(1 - C - D) + (b(1 - C - D) + C + D)]T_{sensor} - DT_a \quad (1)$$



1  
2  
3  
4  
5  
6  
7  
8  
9  
10  
11  
12  
13  
14  
15  
16  
17  
18  
19  
20  
21  
22  
23  
24  
25  
26  
27  
28  
29  
30  
31  
32  
33  
34  
35  
36  
37  
38  
39  
40  
41  
42  
43  
44  
45  
46  
47  
48  
49  
50  
51  
52  
53  
54  
55  
56  
57  
58  
59  
60  
61  
62  
63  
64  
65

161 With  $C = \varepsilon\tau$  ,  $D = (1 - \tau)[1 + (1 - \varepsilon)\tau]$  ,  $a = -67.355351$  and  $b = 0.458606$ , where  $\varepsilon$  land surface  
162 emissivity (LSE) is,  $\tau$  is the total atmospheric transmissivity,  $T_{sensor}$  is the at-sensor brightness  
163 temperature, and  $T_a$  represents the mean atmospheric temperature given by:

$$T_a = 16.011 + 0.92621T_0 \quad (2)$$

167 With  $T_0$  being the near-surface air temperature. Qin et al. (Qin et al., 2001) also estimated the  
168 atmospheric transmissivity from  $w$ , the atmospheric water vapor content, for the range 0.4 to 1.6  
169  $g/cm^2$ , according to the following equations:

$$\tau = 0.97429 - 0.08007 w, \text{ and} \quad (3)$$

$$\tau = 0.982007 - 0.09611 w \quad (4)$$

174 Both  $T_0$  and  $w$  were obtained from local meteorological stations. LSE was obtained from the  
175 NDVI thresholds method (Sobrino et al., 2004).

$$\varepsilon = \varepsilon_{soil}, \text{ when } NDVI < 0.2, \quad (5)$$

$$\varepsilon = \varepsilon_{veg}, \text{ when } NDVI > 0.5 \text{ and} \quad (6)$$

$$\varepsilon = \varepsilon_{veg}P_v + d\varepsilon, \text{ when } 0.2 \geq NDVI \geq 0.5, \quad (7)$$

181 where  $\varepsilon_{soil}$  is the soil emissivity,  $\varepsilon_{veg}$  is the vegetation emissivity, and  $d\varepsilon$  includes the effects of  
182 the geometry of natural surfaces and the internal reflections. Because most of the study area is a

1  
2  
3  
4 183 plain surface, this term is negligible.  $P_v$  is the fraction of the vegetation that can be computed by  
5  
6  
7 184 the following formula (Carlson and Ripley, 1997).  
8

$$P_v = \left[ \frac{NDVI - NDVI_{\min}}{(NDVI_{\max} - NDVI_{\min})} \right]^2 \quad (8)$$

9 185  
10  
11  
12  
13 186  
14  
15  
16 187  
17  
18  
19 188 where,  $NDVI_{\max} = 0.5$ , and  $NDVI_{\min} = 0.2$ . Soil and vegetation emissivities were estimated to be  
20  
21  
22 189 0.97 and 0.99, respectively (Sobrino et al., 2004).  
23  
24 190  
25  
26

### 27 191 *3.2. Spatial Pattern of Green Space*

28  
29 192  
30  
31  
32 193 The multi-spectral Landsat-5 TM data acquired on August 19, 2011 were used to map green  
33  
34 194 space (i.e., vegetated areas) (Fig. 2a). The spatial resolution of the multispectral data is 30 m. A  
35  
36  
37 195 maximum likelihood image classification approach was applied to extract the vegetated area  
38  
39 196 using ENVI from EXELIS Visual Information Solutions. The four bands green, red, near-  
40  
41  
42 197 infrared, and two shortwave infrared were used for classification. An accuracy assessment was  
43  
44 198 conducted based on 200 ground reference data that were photo interpreted from existing land  
45  
46  
47 199 cover map with a scale of 1:150000 (produced by Land Resources Bureau of Aksu City and  
48  
49 200 College of Resources and Environmental Sciences, Xinjiang University, China in June, 2012)  
50  
51 201 together with Landsat true color image. The overall accuracy of the derived classification map  
52  
53  
54 202 was 87.60 %, and the kappa coefficient was 0.83 (Table 1).  
55  
56

1  
2  
3  
4  
5  
6  
7  
8  
9  
10  
11  
12  
13  
14  
15  
16  
17  
18  
19  
20  
21  
22  
23  
24  
25  
26  
27  
28  
29  
30  
31  
32  
33  
34  
35  
36  
37  
38  
39  
40  
41  
42  
43  
44  
45  
46  
47  
48  
49  
50  
51  
52  
53  
54  
55  
56  
57  
58  
59  
60  
61  
62  
63  
64  
65

205  
206  
207  
208  
209  
210  
211  
212  
213  
214  
215  
216  
217  
218  
219  
220  
221  
222  
223  
224  
225  
226  
227

Insert Figure 2 here

Insert Table 1 here

It has been demonstrated that land surface temperature or surface urban heat island could be related to LCLU types (Chen et al., 2006; Connors et al., 2013; Weng, 2001; Xian and Crane, 2006), and there are relationships between spatial structure of urban thermal patterns and urban surface characteristics (Li et al., 2011; Liu and Weng, 2008; Weng et al., 2007). The last several decades have witnessed a remarkable proliferation of studies on developing landscape metrics 1) to characterize landscape patterns and its association to UHIs (Gustafson, 1998; Li and Reynolds, 1993; Li and Wu, 2004; McGarigal and Marks, 1995; Turner, 2005; Turner et al., 1989; Wu, 2000; Wu et al., 2002), and 2) to relate landscape patterns to ecological processes (Turner, 2005). With respect to the measurement objectives, these metrics can be generalized into landscape composition and spatial configuration metrics (Gustafson, 1998; McGarigal and Marks, 1995). Landscape composition metrics measure the presence and amount of different patch types within the landscape without explicitly describing its spatial features while landscape configuration metrics measure the spatial distribution of patches within the landscape (Alberti, 2005). In this study, we selected three commonly occurring landscape metrics to relate LST with spatial pattern of urban green space according to the following principles (Lee et al., 2009; Li and Wu, 2004; Riitters et al., 1995; Riva-Murray et al., 2010): (1) important in both theory and practice, (2) easily calculated, (3) interpretable, and (4) minimal redundancy. Table 2 shows the three landscape metrics. See Mcgarigal et al. (2002) for detailed calculation equation and comments. They are selected to provide complementary information about landscape structure for both composition and configuration.

1  
2  
3  
4 228 Insert Table 2 here  
5  
6  
7 229  
8  
9 230

10 The metrics were calculated using the landscape structure analysis program  
11 FRAGSTATS (<http://www.umass.edu/landeco/research/fragstats/fragstats.html>). The  
12 231 FRAGSTATS software allows the option of conducting a local structure gradient or moving  
13  
14 232 FRAGSTATS software allows the option of conducting a local structure gradient or moving  
15  
16 233 window analysis, and generating the results as a new grid for each selected metric. Our choice  
17  
18  
19 234 was to use moving window analysis, which requires a user specifies the level of heterogeneity  
20  
21 235 (class or landscape) and the shape (round, square or hexagon) and size (radius or length of side,  
22  
23  
24 236 in meters) of the window to be used. A window of the specified shape and size is passed over all  
25  
26 237 positively valued cells inside the landscape of interest. However, only cells in which the entire  
27  
28  
29 238 window is contained within the landscape are evaluated. Within each window, the selected  
30  
31 239 metric at the class or landscape level is computed, and the value is returned to the focal cell. The  
32  
33  
34 240 moving window is passed over the grid until every positively valued cell containing a full  
35  
36 241 window is assessed in this manner.

37  
38 242  
39  
40  
41 243 In our case, we used 8-cell rule which considers all eight adjacent cells that share a side with the  
42  
43 244 focal cell and 500 m-radius circular window. The window moves over the landscape one cell at  
44  
45  
46 245 a time, calculating the selected metric within the window and returning that value to the center  
47  
48 246 cell and output a new continuous surface grid map for each selected metric (Mcgarigal et al.,  
49  
50 247 2002) .

51  
52 248  
53  
54  
55  
56 249 *3.3. Statistical Correlation Measures*  
57  
58 250  
59  
60  
61  
62  
63  
64  
65

1  
2  
3  
4  
5  
6  
7  
8  
9  
10  
11  
12  
13  
14  
15  
16  
17  
18  
19  
20  
21  
22  
23  
24  
25  
26  
27  
28  
29  
30  
31  
32  
33  
34  
35  
36  
37  
38  
39  
40  
41  
42  
43  
44  
45  
46  
47  
48  
49  
50  
51  
52  
53  
54  
55  
56  
57  
58  
59  
60  
61  
62  
63  
64  
65

251 Scatter plots were generated to explore the bivariate relationship between LST and each of the  
252 landscape metrics. The normalized mutual information measure was assessed based on them  
253 (Cover and Thomas, 1991; Webb, 2002). The Shannon entropy of a continuous random variable  
254  $X$  with probability density function  $p(x)$  for all possible events  $x \in S$  is defined as

$$H(X) = - \int_S p(x) \log p(x) dx \quad (9)$$

255 where  $S$  is the support of the variable and  $p(x)$  is its probability distribution function. Probability  
256 distributions may be used to construct a frequency distribution of certain events occurring either  
257 discretely, in the form of a histogram, or continuously (Allaby, 2008).

260 In the case of a discrete random variable  $X$ , entropy  $H(X)$  is expressed as

$$H(X) = - \sum_{x \in \Omega} p(x) \log p(x) \quad (10)$$

264 where  $p(x)$  represents the probability of an event  $x \in \Omega$  from a finite set ( $\Omega$ ) of possible values.

266 In probability and information theories, the mutual information of two random  
267 variables is a quantity that measures the amount of information that both variables share.

268 Formally, the mutual information of two discrete random variables  $X$  and  $Y$  can be defined as:

$$I(X, Y) = \sum_{x \in X} \sum_{y \in Y} p(x, y) \log \left( \frac{p(x, y)}{p(x)p(y)} \right) \quad (11)$$

1  
2  
3  
4 270  
5  
6  
7 271  
8  
9 272  
10  
11  
12 273  
13  
14 274  
15  
16 275  
17  
18  
19 276  
20  
21 277  
22  
23  
24 278  
25  
26 279  
27  
28  
29 280  
30  
31 281  
32  
33  
34 282  
35  
36 283  
37  
38  
39 284  
40  
41 285  
42  
43 286  
44  
45  
46 287  
47  
48  
49  
50  
51  
52 288  
53  
54  
55 289  
56  
57 290  
58  
59  
60 291  
61  
62  
63  
64  
65

where  $p(x, y)$  is the joint probability function of  $X$  and  $Y$ , defined as

$$p(x, y) = P(X = x \& Y = y) \quad (12)$$

We can define:

$$p(x) = \sum_{y \in A} p(X = x, y) \quad (13)$$

$$p(y) = \sum_{x \in A} p(x, Y = y) \quad (14)$$

as the marginal probability distribution functions of  $X$  and  $Y$  respectively.

$I(x, y)$  is always a non-negative quantity, being zero when the variables are statistically independent. The higher the value of  $I$ , the higher is the dependence between them.

The normalized mutual information (Cover and Thomas, 1991; Sridhar et al., 1998), can be defined as

$$C_{XY} = \frac{I(X; Y)}{H(Y)} \text{ and } C_{YX} = \frac{I(X; Y)}{H(X)} \quad (15)$$

This expression can be used as a “correlation” measure (Cover and Thomas, 1991) with the advantage of capturing linear and non-linear relationships among variables. It is sometimes called as “asymmetric dependency coefficient (ADC)” (Sridhar et al., 1998). However, two

1  
2  
3  
4 292 definitions in Eq. (15) will produce unequal values due to their asymmetric property in the  
5  
6  
7 293 definitions. Therefore, a symmetric normalized mutual information measure can be proposed  
8  
9 294 (Press et al., 1990; Strehl and Ghosh, 2003), such as

$$NI(X, Y) = 2 \frac{I(X, Y)}{H(Y) + H(X)}, NI(X, Y) = \frac{I(X, Y)}{\sqrt{H(Y)H(X)}} \quad (16)$$

10  
11 295  
12  
13  
14  
15  
16  
17  
18 296  
19  
20  
21 297 It is worth mentioning that the mutual information of two random variables  $I(X, Y)$  is always  
22  
23 298 smaller than the entropy of any of them, i. e.,  $H(X)$  or  $H(Y)$ , namely:  $I(X; Y) < H(Y)$  and  
24  
25  
26 299  $I(X; Y) < H(X)$  are valid, because the information both variables share can never be greater than  
27  
28 300 the information each one has. Therefore  $0 \leq C_{XY} \leq 1$ . If  $C_{XY}$  equals one, it means  $X, Y$  are  
29  
30  
31 301 perfectly correlated. If  $C_{XY}$  equals 0 it indicates there is no correlation between  $X, Y$ .

32  
33 302  
34  
35 303 In this study, Eq. 15 was applied to measure the normalized mutual information between the  
36  
37  
38 304 different variables since the focus of the work is to find out the correlation between the land  
39  
40  
41 305 surface temperature, which is chosen as a proxy of target variable, and other variables including  
42  
43 306 PLAND, PD and ED.

#### 46 307 **4. Results**

47  
48 308  
49  
50 309 The spatial distribution of PLAND is shown in (Fig. 3a), PD (Fig. 3b) and ED (Fig. 3c). Higher  
51  
52  
53 310 vegetation cover or percent green space is located on the eastern edge of the study site, which is  
54  
55  
56 311 possibly a park or a nursery with mature grown trees (Fig. 3a). Patch density is high over the  
57  
58 312 Middle-Western Aksu downtown (Fig. 3b) indicating more fragmented but evenly distributed  
59  
60  
61  
62  
63  
64  
65

1  
2  
3  
4  
5  
6  
7  
8  
9  
10  
11  
12  
13  
14  
15  
16  
17  
18  
19  
20  
21  
22  
23  
24  
25  
26  
27  
28  
29  
30  
31  
32  
33  
34  
35  
36  
37  
38  
39  
40  
41  
42  
43  
44  
45  
46  
47  
48  
49  
50  
51  
52  
53  
54  
55  
56  
57  
58  
59  
60  
61  
62  
63  
64  
65

313 vegetation patches. Edge density, an indicator of linear configuration of green space along the  
314 streets, appears to be large on southwest and northeast parts of the study site. The spatial  
315 distribution patterns of patch density and edge density are similar suggesting there exists some  
316 degree of correlation between these two variables.

317 Insert Figure 3 here

318  
319 Two dimensional scatter plots between LST and landscape metrics are shown in Fig. 4. There  
320 seems to be a negative linear relationship between LST and both vegetation fraction and edge  
321 density. However, these relationships do not seem to be statistically significant enough ( $R^2 <$   
322  $0.32$  in all cases) to obtain meaningful conclusions. That is why other measures may play an  
323 important role. However, some useful information can be extracted. It is interesting to note that  
324 patch density and edge density are correlated variables but demonstrates very different degrees  
325 of effects on LST. The results imply that edge density has more deterministic effects on LST  
326 than the patch density. One may expect that plantation of street trees evenly distributed in the  
327 urban area may be an effective way of reducing urban heat island effects, therefore, energy  
328 consumption as opposed to establishing dense patches of green space in discrete locations.

329  
330 Insert Figure 4 here

331  
332 Table 3 shows the normalized mutual information analysis between the LST and landscape  
333 metrics calculated using Eq. (15). It is evident that the compositional and spatial configuration of  
334 urban green space can affect the LST to a certain degree. When these two major categories of  
335 green space pattern are taken into account separately, it seems the compositional green space



1  
2  
3  
4 336 pattern has slightly larger effect on LST than configurational factors. Meanwhile, the  
5  
6  
7 337 configurational green space patterns do have relatively strong effect but not as strong as  
8  
9 338 compositional green space pattern. The mutual information value was largest when all three  
10  
11 339 landscape metrics were considered in order to see the effect on the LST. This is expected since  
12  
13  
14 340 each of the landscape metrics does have some level of causal interactions with LST change, and  
15  
16 341 the effects could constructively interfere each other. Combination of any two or three of the  
17  
18  
19 342 landscape metrics had a higher impact on LST than that of a single variable. The joint effect of  
20  
21 343 (*PLAND*, *PD*) was slightly better in magnitude than the effect of (*PLAND*, *ED*) on LST,  
22  
23  
24 344 confirming the stronger correlation between edge density and LST as shown in Fig. 4. However,  
25  
26 345 the mutual information value between (*ED*, *PD*) and LST was larger than of the (*PLAND*, *PD*)  
27  
28  
29 346 and (*PLAND*, *ED*), which might be attributed to the fact that 1) patch density and edge density is  
30  
31 347 more determinative factors that elicits LST, and 2) there exist correlations between patch density  
32  
33 348 and edge density.

35  
36 349 Insert Table 3 here  
37  
38

39 350 **5. Discussion**  
40  
41 351

42  
43  
44 352 The results of this study showed that *PLAND* was correlated with LST with statistical  
45  
46 353 significance. This is consistent with a number of previous studies, which demonstrated negative  
47  
48  
49 354 correlations between LST and the abundance of green space measured by Normalized Difference  
50  
51 355 Vegetation Index (Buyantuyev and Wu, 2010; Chen et al., 2006), fraction of vegetation (Weng et  
52  
53  
54 356 al., 2004), percent cover of LCLU (e.g., Forest, Grass, Cropland, etc.) (Weng et al., 2006; Zhou  
55  
56 357 et al., 2011), or *PLAND* (Li et al., 2012). Trees and other plants help cool the environment,  
57  
58 358 making green space a simple and effective way to mitigate urban heat island effects. Green  
59  
60  
61  
62  
63  
64  
65

1  
2  
3  
4 359 spaces lower surface and air temperatures by evapotranspiration due to its lower thermal inertia  
5  
6  
7 360 compared to impervious surfaces and bare soils (Hamada and Ohta, 2010; Lambin and Ehrlich,  
8  
9 361 1996; Weng et al., 2004); by providing shade that prevents land surfaces from direct heating  
10  
11 362 from sunlight (Zhou et al., 2011). Concerning the configurational metrics, the PD and ED were  
12  
13  
14 363 less correlated with LST than PLAND. The normalized mutual information analysis also showed  
15  
16 364 that there was less dependence between the LST with individual PD and ED, which is still  
17  
18  
19 365 smaller than the dependence between the PLAND and LST. This indicates that the increase of  
20  
21 366 patch density leads to a decrease in mean patch size resulting in a general increase in total patch  
22  
23  
24 367 edges. Therefore, the effects of the increase in patch density on LST can be explained by both a  
25  
26 368 decrease in mean patch size and increase in patch edges. The decrease in mean patch size may  
27  
28  
29 369 increase LST because a larger, continuous green space produces stronger cool island effects than  
30  
31 370 that of several small pieces of green space even if whose total area equals to the area of the  
32  
33 371 continuous green space (Cao et al., 2010; Li et al., 2012; Zhang et al., 2009). In contrast, the  
34  
35  
36 372 increase of total patch edges may enhance energy flow and exchange between green space and  
37  
38 373 its surrounding areas, and provide more shade for surrounding surfaces, which lead to the  
39  
40  
41 374 decrease of LST (Zhou et al., 2011).

42  
43 375  
44  
45  
46 376 As far as the each landscape metric is concerned individually, the highest normalized  
47  
48 377 mutual information measure was found with the PLAND (0.71). The implication from this  
49  
50  
51 378 observation is that the composition of green space was more important than the configuration of  
52  
53 379 green space in reducing UHI effects, which is consistent with previous findings (Li et al., 2012;  
54  
55 380 Zhou et al., 2011). However, our results also showed that ED and PD together were the most  
56  
57  
58 381 deterministic factors of LST than the unique effects of a single variable or the joint effects

1  
2  
3  
4  
5  
6  
7  
8  
9  
10  
11  
12  
13  
14  
15  
16  
17  
18  
19  
20  
21  
22  
23  
24  
25  
26  
27  
28  
29  
30  
31  
32  
33  
34  
35  
36  
37  
38  
39  
40  
41  
42  
43  
44  
45  
46  
47  
48  
49  
50  
51  
52  
53  
54  
55  
56  
57  
58  
59  
60  
61  
62  
63  
64  
65

382 PLAND and PD or PLAND and ED. Normalized mutual information measure between LST and  
383 PLAND and ED, PLAND and PD and ED and PD were 0.7679, 0.7650 and 0.7832, respectively.  
384 A combination of the three factors PLAND, PD and ED explained much of the variance of LST  
385 with a normalized mutual information measure of 0.8694. This is because the composition and  
386 configuration of green space are constructively interrelated.

387 Many of the results from this study regarding to the relationships between the green space  
388 and LST were expected as reported in a number of publications (Connors et al., 2013; Hamada  
389 and Ohta, 2010; Li et al., 2011; Weng et al., 2004). Traditionally, increasing the green space by  
390 planting more trees has been emphasized in urban planning (Rizwan et al., 2008a; Zhou et al.,  
391 2011). While confirming the fact that the increase in green space can significantly mitigate UHI  
392 effects, our results showed that configuration of green space as expressed by the joint effect of  
393 PD and ED is the most deterministic metric that affects LST. Optimizing the configuration of  
394 green space which increases the PD and ED should be highlighted to mitigate UHI effects. These  
395 results have important implications for green space management, particularly in rapidly  
396 urbanizing arid regions as in our case study, where both water resources and available land area  
397 for increased green space is extremely limited.

398 Under changing climate, arid regions are likely to become even drier, while wet areas  
399 tend to get wetter in response to observed global warming (Durack et al., 2012) as indicated by  
400 increasing surface temperature. Expanding the urban green space is a rational approach for  
401 adapting to climate change. At the same time, it can contribute to the sustainable development of  
402 urban areas. However, it may compete with other socio-economic interests that also require  
403 space. Therefore, in order to determine a proper balance between the sustainable development  
404 and urban green space increase, urban planners should work on optimizing the configuration of

1  
2  
3  
4  
5  
6  
7  
8  
9  
10  
11  
12  
13  
14  
15  
16  
17  
18  
19  
20  
21  
22  
23  
24  
25  
26  
27  
28  
29  
30  
31  
32  
33  
34  
35  
36  
37  
38  
39  
40  
41  
42  
43  
44  
45  
46  
47  
48  
49  
50  
51  
52  
53  
54  
55  
56  
57  
58  
59  
60  
61  
62  
63  
64  
65

405 green space patches in selected areas by increasing the size of existing green space patches rather  
406 than building new smaller patches. In the arid Northwestern China, where temperatures are  
407 already high and water resources are limited, the outcome of this study can support decisions  
408 about sustainable urban design and development, which will help mitigating the effects of future  
409 climate, and benefit human wellbeing by improving water and energy use efficiency.

**6. Conclusion**

411  
412 Taking the urban area of the oasis city of Aksu area as an example, this study  
413 quantitatively examined the effects of spatial composition and configuration of green space on  
414 land surface temperature (LST). Normalized mutual information measure was used to quantify  
415 the relationship between LST and landscape metrics including percentage of landscape  
416 (PLAND), edge density (ED) and patch density (PD). Our results showed that 1) both the  
417 composition and configuration of green space elicits urban heat island; 2) joint effects of any two  
418 combinations of the metrics was larger than the effect of a single metric; 3) ED and PD  
419 combined was the most deterministic factor of LST than the unique effects of a single variable or  
420 the joint effects PLAND and PD or PLAND and ED; 4) optimizing the configuration of green  
421 space which increases the PD and ED should be prioritized in sustainable urban planning and  
422 development to mitigate urban heat island effects.

423 Water scarcity is the major limiting factor of anthropogenic activities in arid and semi-  
424 arid regions. Specifically, the increase of green space cover is restricted by water availability.  
425 Our results suggested that by increasing patch and edge density of the green space, the thermal  
426 environment in the City of Aksu can be further improved without expanding the percentage of  
427 landscape (PLAND). In arid and semi-arid regions, where temperatures are already high and

1  
2  
3  
4  
5  
6  
7  
8  
9  
10  
11  
12  
13  
14  
15  
16  
17  
18  
19  
20  
21  
22  
23  
24  
25  
26  
27  
28  
29  
30  
31  
32  
33  
34  
35  
36  
37  
38  
39  
40  
41  
42  
43  
44  
45  
46  
47  
48  
49  
50  
51  
52  
53  
54  
55  
56  
57  
58  
59  
60  
61  
62  
63  
64  
65

428 water resources are limited, the outcome of this study may provide climate change adaptation  
429 and mitigation benefits by reducing greenhouse gas emissions and energy demand for the  
430 cooling of buildings.

431  
432 **Acknowledgments**

433  
434 The first author would like to express his gratitude to the European Commission and Erasmus  
435 Mundus Consortium for their important scholarship for master students. We acknowledge the  
436 National Natural Science Foundation of China (#s: 31270742, U1138303, 41130531, 41361016),  
437 Sino-German joint research project SuMaRiO (01LL0918C), Research Foundation of Xinjiang  
438 University (BS120116 and XY110117) and Education Department of Xinjiang  
439 Uygur Autonomous Region (XJEDU2011S07) for financially supporting this work. Finally, we  
440 also extend our gratitude to the anonymous reviewers of this manuscript for their helpful  
441 suggestions.

442 **References**

443  
444 Alberti, M., 2005. The effects of urban patterns on ecosystem function. International regional  
445 science review 28, 168-192.  
446 Allaby, M., 2008. A Dictionary of Earth Sciences, Third ed. Oxford University Press Inc., New  
447 York, pp: 460  
448 Arnfield, A.J., 2003. Two decades of urban climate research: a review of turbulence, exchanges  
449 of energy and water, and the urban heat island. International Journal of Climatology 23,  
450 1-26.

1  
2  
3  
4 451 Baker, L.A., Brazel, A.J., Westerhoff, P., 2004. Environmental consequences of rapid  
5  
6  
7 452 urbanization in warm, arid lands: case study of Phoenix, Arizona (USA). In: Marchettini  
8  
9 453 N, Brebbia C, Tiezzi E, Wadhwa LC (eds) The sustainable city III, (Proceedings of the  
10  
11 454 Sienna Conference, held June 2004), Advances in Architecture Series, WIT Press,  
12  
13  
14 455 Boston.

15  
16 456 Bowler, D.E., Buyung-Ali, L., Knight, T.M., Pullin, A.S., 2010. Urban greening to cool towns  
17  
18  
19 457 and cities: A systematic review of the empirical evidence. *Landscape and Urban Planning*  
20  
21 458 97, 147-155.

22  
23  
24 459 Buyantuyev, A., Wu, J., 2010. Urban heat islands and landscape heterogeneity: linking  
25  
26 460 spatiotemporal variations in surface temperatures to land-cover and socioeconomic  
27  
28  
29 461 patterns. *Landscape ecology* 25, 17-33.

30  
31 462 Cao, X., Onishi, A., Chen, J., Imura, H., 2010. Quantifying the cool island intensity of urban  
32  
33  
34 463 parks using ASTER and IKONOS data. *Landscape and Urban Planning* 96, 224-231.

35  
36 464 Carlson, T.N., Ripley, D.A., 1997. On the relation between NDVI, fractional vegetation cover,  
37  
38 465 and leaf area index. *Remote Sensing of Environment* 62, 241-252.

39  
40  
41 466 Chen, X.L., Zhao, H.M., Li, P.X., Yin, Z.Y., 2006. Remote sensing image-based analysis of the  
42  
43 467 relationship between urban heat island and land use/cover changes. *Remote Sensing of*  
44  
45  
46 468 *Environment* 104, 133-146.

47  
48 469 Connors, J.P., Galletti, C.S., Chow, W.T.L., 2013. Landscape configuration and urban heat  
49  
50  
51 470 island effects: assessing the relationship between landscape characteristics and land  
52  
53 471 surface temperature in Phoenix, Arizona. *Landscape Ecology*, 28, 271-283.

54  
55 472 Cover, T., Thomas, J., 1991. *Elements of Information Theory*. Wiley-Interscience.

1  
2  
3  
4  
5  
6  
7  
8  
9  
10  
11  
12  
13  
14  
15  
16  
17  
18  
19  
20  
21  
22  
23  
24  
25  
26  
27  
28  
29  
30  
31  
32  
33  
34  
35  
36  
37  
38  
39  
40  
41  
42  
43  
44  
45  
46  
47  
48  
49  
50  
51  
52  
53  
54  
55  
56  
57  
58  
59  
60  
61  
62  
63  
64  
65

473 Cui, Y.Y., de Foy, B., 2012. Seasonal Variations of the Urban Heat Island at the surface and the  
474 near-surface and reductions due to urban vegetation in Mexico City. *Journal of Applied  
475 Meteorology and Climatology*, 51, 855–868.

476 Dousset, B., Gourmelon, F., 2003. Satellite multi-sensor data analysis of urban surface  
477 temperatures and landcover. *ISPRS Journal of Photogrammetry and Remote Sensing* 58,  
478 43-54.

479 Durack, P.J., Wijffels, S.E., Matear, R.J., 2012. Ocean Salinities Reveal Strong Global Water  
480 Cycle Intensification During 1950 to 2000. *Science* 336, 455-458.

481 Fan, P., Qi, J., 2010. Assessing the sustainability of major cities in China. *Sustainability Science*,  
482 5, 51-68.

483 Feizizadeh, B., Blaschke, T., 2013. Examining urban heat island relations to land use and air  
484 pollution: multiple endmember spectral mixture analysis for thermal remote sensing.  
485 *IEEE Journal of Selected Topics in Applied Earth Observations and Remote Sensing*, 6,  
486 1749-1756.

487 Gustafson, E.J., 1998. Quantifying landscape spatial pattern: What is the state of the art?  
488 *Ecosystems* 1, 143-156.

489 Halik, W., Mamat, A., Dang, J.H., Deng, B.S.H., Tiyyip, T., 2013. Suitability analysis of human  
490 settlement environment within the Tarim Basin in Northwestern China. *Quaternary  
491 International*, 311, 175-180.

492 Hamada, S., Ohta, T., 2010. Seasonal variations in the cooling effect of urban green areas on  
493 surrounding urban areas. *Urban forestry & urban greening* 9, 15-24.

494 Hamdi, R., Schayes, G., 2007. Sensitivity study of the urban heat island intensity to urban  
495 characteristics. *International Journal of Climatology* 28, 973-982.

1  
2  
3  
4  
5  
6  
7  
8  
9  
10  
11  
12  
13  
14  
15  
16  
17  
18  
19  
20  
21  
22  
23  
24  
25  
26  
27  
28  
29  
30  
31  
32  
33  
34  
35  
36  
37  
38  
39  
40  
41  
42  
43  
44  
45  
46  
47  
48  
49  
50  
51  
52  
53  
54  
55  
56  
57  
58  
59  
60  
61  
62  
63  
64  
65

496 Honjo, T., Takakura, T., 1991. Simulation of thermal effects of urban green areas on their  
497 surrounding areas. *Energy and Buildings* 15, 443-446.

498 Howard, L., 1818. *The climate of London, deduced from Meteorological observations, made at*  
499 *different places in the neighbourhood of the metropolis, vol. 2*, London, 1818-20.

500 Huang, G., Zhou, W., Cadenasso, M.L., 2011. Is everyone hot in the city? Spatial pattern of land  
501 surface temperatures, land cover and neighborhood socioeconomic characteristics in  
502 Baltimore, MD. *Journal of Environmental Management*, 92,1753-1759.

503 Imhoff, M.L., Zhang, P., Wolfe, R.E., Bounoua, L., 2010. Remote sensing of the urban heat  
504 island effect across biomes in the continental USA. *Remote Sensing of Environment*  
505 114, 504-513.

506 James, W., 2002. Green roads: research into permeable pavers. *Stormwater* 3, 48-40.

507 Lai, L.-W., Cheng, W.-L., 2009. Air quality influenced by urban heat island coupled with  
508 synoptic weather patterns. *Science of The Total Environment* 407, 2724-2733.

509 Lambin, E., Ehrlich, D., 1996. The surface temperature-vegetation index space for land cover  
510 and land-cover change analysis. *International Journal of Remote Sensing* 17, 463-487.

511 Lee, S.-W., Hwang, S.-J., Lee, S.-B., Hwang, H.-S., Sung, H.-C., 2009. Landscape ecological  
512 approach to the relationships of land use patterns in watersheds to water quality  
513 characteristics. *Landscape and Urban Planning* 92, 80-89.

514 Li, H., Reynolds, J.F., 1993. A new contagion index to quantify spatial patterns of landscapes.  
515 *Landscape ecology* 8, 155-162.

516 Li, H., Wu, J., 2004. Use and misuse of landscape indices. *Landscape ecology* 19, 389-399.



1  
2  
3  
4 517 Li, J., Song, C., Cao, L., Zhu, F., Meng, X., Wu, J., 2011. Impacts of landscape structure on  
5  
6 518 surface urban heat islands: A case study of Shanghai, China. *Remote Sensing of*  
7  
8  
9 519 *Environment* 115, 3249-3263.  
10  
11 520 Li, X., Zhou, W., Ouyang, Z., Xu, W., Zheng, H., 2012. Spatial pattern of greenspace affects  
12  
13  
14 521 land surface temperature: evidence from the heavily urbanized Beijing metropolitan area,  
15  
16 522 China. *Landscape Ecology*, 27, 887-898.  
17  
18  
19 523 Li, X., Zhou W., Ouyang, Z., 2013. Relationship between land surface temperature and spatial  
20  
21 524 pattern of greenspace: What are the effects of spatial resolution? *Landscape and Urban*  
22  
23 525 *Planning*, 114, 1-8.  
24  
25  
26 526 Liu, G., Kurban, A., Duan, H., Halik, Ü., Ablekim, A., Zhang, L. Desert riparian forest  
27  
28 527 colonization in the lower reaches of Tarim River based on remote sensing analysis.  
29  
30 528 *Environmental Earth Sciences*, DOI: 10.1007/s12665-013-2850-9.  
31  
32  
33 529 Liu, H., Weng, Q., 2008. Seasonal variations in the relationship between landscape pattern and  
34  
35 530 land surface temperature in Indianapolis, USA. *Environmental Monitoring Assessment*,  
36  
37 531 144, 199-219.  
38  
39  
40 532 Mcgarigal, K., Cushman, S., Neel, M., Ene, E., 2002. FRAGSTATS: spatial pattern analysis  
41  
42 533 program for categorical maps.  
43  
44  
45 534 McGarigal, K., Marks, B.J., 1995. Spatial pattern analysis program for quantifying landscape  
46  
47 535 structure. Gen. Tech. Rep. PNW-GTR-351. US Department of Agriculture, Forest  
48  
49 536 Service, Pacific Northwest Research Station.  
50  
51  
52 537 Niemelä, J., 1999. Ecology and urban planning. *Biodiversity and conservation* 8, 119-131.  
53  
54  
55 538 Patz, J.A., Campbell-Lendrum, D., Holloway, T., Foley, J.A., 2005. Impact of regional climate  
56  
57 539 change on human health. *Nature* 438, 310-317.  
58  
59  
60  
61  
62  
63  
64  
65

1  
2  
3  
4  
5  
6  
7  
8  
9  
10  
11  
12  
13  
14  
15  
16  
17  
18  
19  
20  
21  
22  
23  
24  
25  
26  
27  
28  
29  
30  
31  
32  
33  
34  
35  
36  
37  
38  
39  
40  
41  
42  
43  
44  
45  
46  
47  
48  
49  
50  
51  
52  
53  
54  
55  
56  
57  
58  
59  
60  
61  
62  
63  
64  
65

540 Press, W.H., Flannery, B.P., Teukolsky, S.A., Vetterling, W.T., 1990. Numerical recipes.  
541 Cambridge Univ Press.

542 Pu, R., Gong, P., Michishita, R., Sasagawa, T., 2006. Assessment of multi-resolution and multi-  
543 sensor data for urban surface temperature retrieval. Remote Sensing of Environment 104,  
544 211-225.

545 Qin, Z.-h., Karnieli, A., Berliner, P., 2001. A mono-window algorithm for retrieving land surface  
546 temperature from Landsat TM data and its application to the Israel-Egypt border region.  
547 International Journal of Remote Sensing 22, 3719-3746.

548 Riitters, K.H., O'Neill, R., Hunsaker, C., Wickham, J.D., Yankee, D., Timmins, S., Jones, K.,  
549 Jackson, B., 1995. A factor analysis of landscape pattern and structure metrics.  
550 Landscape ecology 10, 23-39.

551 Riva-Murray, K., Riemann, R., Murdoch, P., Fischer, J.M., Brightbill, R., 2010. Landscape  
552 characteristics affecting streams in urbanizing regions of the Delaware River Basin (New  
553 Jersey, New York, and Pennsylvania, US). Landscape ecology 25, 1489-1503.

554 Rizwan, A.M., Dennis, L.Y., Liu, C., 2008a. A review on the generation, determination and  
555 mitigation of Urban Heat Island. Journal of Environmental Sciences 20, 120-128.

556 Rizwan, A.M., Dennis, L.Y.C., Liu, C., 2008b. A review on the generation, determination and  
557 mitigation of Urban Heat Island. Journal of Environmental Sciences 20, 120-128.

558 Sarrat, C., Lemonsu, A., Masson, V., Guedalia, D., 2006. Impact of urban heat island on regional  
559 atmospheric pollution. Atmospheric Environment 40, 1743-1758.

560 Sobrino, J.A., Jiménez-Muñoz, J.C., Paolini, L., 2004. Land surface temperature retrieval from  
561 LANDSAT TM 5. Remote Sensing of Environment 90, 434-440.

1  
2  
3  
4  
5  
6  
7  
8  
9  
10  
11  
12  
13  
14  
15  
16  
17  
18  
19  
20  
21  
22  
23  
24  
25  
26  
27  
28  
29  
30  
31  
32  
33  
34  
35  
36  
37  
38  
39  
40  
41  
42  
43  
44  
45  
46  
47  
48  
49  
50  
51  
52  
53  
54  
55  
56  
57  
58  
59  
60  
61  
62  
63  
64  
65

562 Sridhar, D.V., Bartlett, E.B., Seagrave, R.C., 1998. Information theoretic subset selection for  
563 neural network models. *Computers & chemical engineering* 22, 613-626.

564 Strehl, A., Ghosh, J., 2003. Cluster ensembles---a knowledge reuse framework for combining  
565 multiple partitions. *The Journal of Machine Learning Research* 3, 583-617.

566 Taha, H., 1997. Urban climates and heat islands: albedo, evapotranspiration, and anthropogenic  
567 heat. *Energy and buildings* 25, 99-103.

568 Tran, H., Uchihama, D., Ochi, S., Yasuoka, Y., 2006. Assessment with satellite data of the urban  
569 heat island effects in Asian mega cities. *International Journal of Applied Earth  
570 Observation and Geoinformation* 8, 34-48.

571 Turner, M.G., 2005. Landscape ecology: what is the state of the science? *Annual Review of  
572 Ecology, Evolution, and Systematics*, 319-344.

573 Turner, M.G., O'Neill, R.V., Gardner, R.H., Milne, B.T., 1989. Effects of changing spatial scale  
574 on the analysis of landscape pattern. *Landscape ecology* 3, 153-162.

575 Unger, J., 2004. Intra-urban relationship between surface geometry and urban heat island: review  
576 and new approach. *Climate research* 27, 253-264.

577 Voogt, J.A., Oke, T., 1998. Effects of urban surface geometry on remotely-sensed surface  
578 temperature. *International Journal of Remote Sensing* 19, 895-920.

579 Voogt, J.A., Oke, T.R., 2003. Thermal remote sensing of urban climates. *Remote sensing of  
580 Environment* 86, 370-384.

581 Solecki, W.D., Rosenzweig, C., Parshall, L., Pope, G., Clark, M., Cox, J., Wiencke, M., 2005.  
582 Mitigation of the heat island effect in urban New Jersey. *Global Environmental Change  
583 Part B: Environmental Hazards*, 6, 39-49.

584 Webb, A.R., 2002. *Statistical pattern recognition*. Wiley.

1  
2  
3  
4 585 Weng, Q., 2001. A remote sensing? GIS evaluation of urban expansion and its impact on surface  
5  
6 586 temperature in the Zhujiang Delta, China. *International Journal of Remote Sensing* 22,  
7  
8  
9 587 1999-2014.

10  
11 588 Weng, Q., 2009. Thermal infrared remote sensing for urban climate and environmental studies:  
12  
13  
14 589 Methods, applications, and trends. *ISPRS Journal of Photogrammetry and Remote*  
15  
16 590 *Sensing* 64, 335-344.

17  
18  
19 591 Weng, Q., Liu, H., Lu, D., 2007. Assessing the effects of land use and land cover patterns on  
20  
21 592 thermal conditions using landscape metrics in city of Indianapolis, United States. *Urban*  
22  
23  
24 593 *Ecosystems* 10, 203-219.

25  
26 594 Weng, Q., Lu, D., Liang, B., 2006. Urban surface biophysical descriptors and land surface  
27  
28 595 temperature variations. *Photogrammetric Engineering & Remote Sensing* 72, 1275-1286.

29  
30  
31 596 Weng, Q., Lu, D., Schubring, J., 2004. Estimation of land surface temperature–vegetation  
32  
33 597 abundance relationship for urban heat island studies. *Remote sensing of Environment* 89,  
34  
35  
36 598 467-483.

37  
38 599 Weng, Q., Yang, S., 2006. Urban Air Pollution Patterns, Land Use, and Thermal Landscape: An  
39  
40  
41 600 Examination of the Linkage Using GIS. *Environ Monit Assess* 117, 463-489.

42  
43 601 Wu, C-D., Lung, S-C. C., Jan, J-F., 2013. Development of a 3-D urbanization index using digital  
44  
45  
46 602 terrain models for surface urban heat island effects. *ISPRS Journal of Photogrammetry*  
47  
48 603 *and Remote Sensing*, 81, 1-11.

49  
50 604 Wu, J., 2000. *Landscape ecology: pattern, process, scale and hierarchy*. Beijing: Higher  
51  
52  
53 605 Education Press 13, 121-123.

54  
55 606 Wu, J., Shen, W., Sun, W., Tueller, P.T., 2002. Empirical patterns of the effects of changing  
56  
57  
58 607 scale on landscape metrics. *Landscape Ecology* 17, 761-782.

59  
60  
61  
62  
63  
64  
65

1  
2  
3  
4  
5  
6  
7  
8  
9  
10  
11  
12  
13  
14  
15  
16  
17  
18  
19  
20  
21  
22  
23  
24  
25  
26  
27  
28  
29  
30  
31  
32  
33  
34  
35  
36  
37  
38  
39  
40  
41  
42  
43  
44  
45  
46  
47  
48  
49  
50  
51  
52  
53  
54  
55  
56  
57  
58  
59  
60  
61  
62  
63  
64  
65

608 Xian, G., Crane, M., 2006. An analysis of urban thermal characteristics and associated land  
609 cover in Tampa Bay and Las Vegas using Landsat satellite data. *Remote Sensing of*  
610 *Environment* 104, 147-156.

611 Yokohari, M., Brown, R.D., Kato, Y., Moriyama, H., 1997. Effects of paddy fields on  
612 summertime air and surface temperatures in urban fringe areas of Tokyo, Japan.  
613 *Landscape and urban planning* 38, 1-11.

614 Zhang, X., Zhong, T., Feng, X., Wang, K., 2009. Estimation of the relationship between  
615 vegetation patches and urban land surface temperature with remote sensing. *International*  
616 *Journal of Remote Sensing* 30, 2105-2118.

617 Zhao, C., Fu, G., Liu, X., Fu, F., 2011. Urban planning indicators, morphology and climate  
618 indicators: A case study for a north-south transect of Beijing, China. *Building and*  
619 *Environment* 46, 1174-1183.

620 Zhou, W., Huang, G., Cadenasso, M.L., 2011. Does spatial configuration matter? Understanding  
621 the effects of land cover pattern on land surface temperature in urban landscapes.  
622 *Landscape and Urban Planning* 102, 54-63.

623  
624  
625  
626  
627  
628  
629

1  
2  
3  
4  
5  
6  
7  
8  
9  
10  
11  
12  
13  
14  
15  
16  
17  
18  
19  
20  
21  
22  
23  
24  
25  
26  
27  
28  
29  
30  
31  
32  
33  
34  
35  
36  
37  
38  
39  
40  
41  
42  
43  
44  
45  
46  
47  
48  
49  
50  
51  
52  
53  
54  
55  
56  
57  
58  
59  
60  
61  
62  
63  
64  
65

**Tables:**

**Table 1** Accuracy assessment of the urban green space classification map

**Table 2** Landscape metrics used in this study(Mcgarigal et al., 2002)

**Table 3** Normalized mutual information results of compositional configuration of green space and landscape metrics

**Figures:**

**Fig. 1.** Location map of the study area showing overview map of China (top - left corner) and the Xinjiang Uyghur Autonomous Region (bottom-left corner).

**Fig. 2.** Green space and LST maps for the downtown are Aksu city: (a) green space map, and (b) LST map with units of Kelvin

**Fig. 3.** Grid map of urban green space metrics (a) Percent cover of green space (b) Patch density (c) Edge density

**Fig. 4.** Scatter plot of LST with PLAND, PD and ED

Figure 1  
Click here to download high resolution image

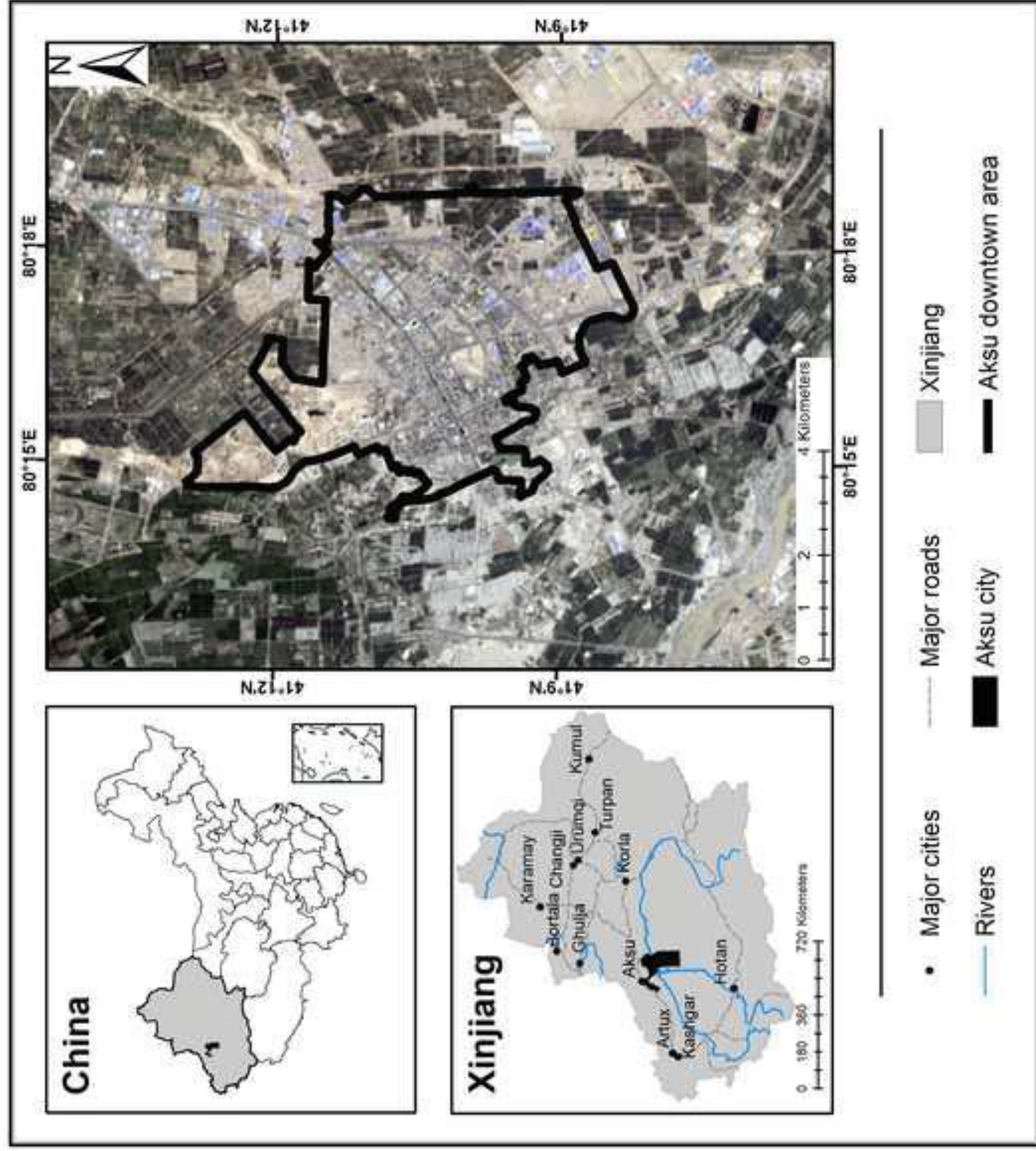




Figure 2  
[Click here to download high resolution image](#)

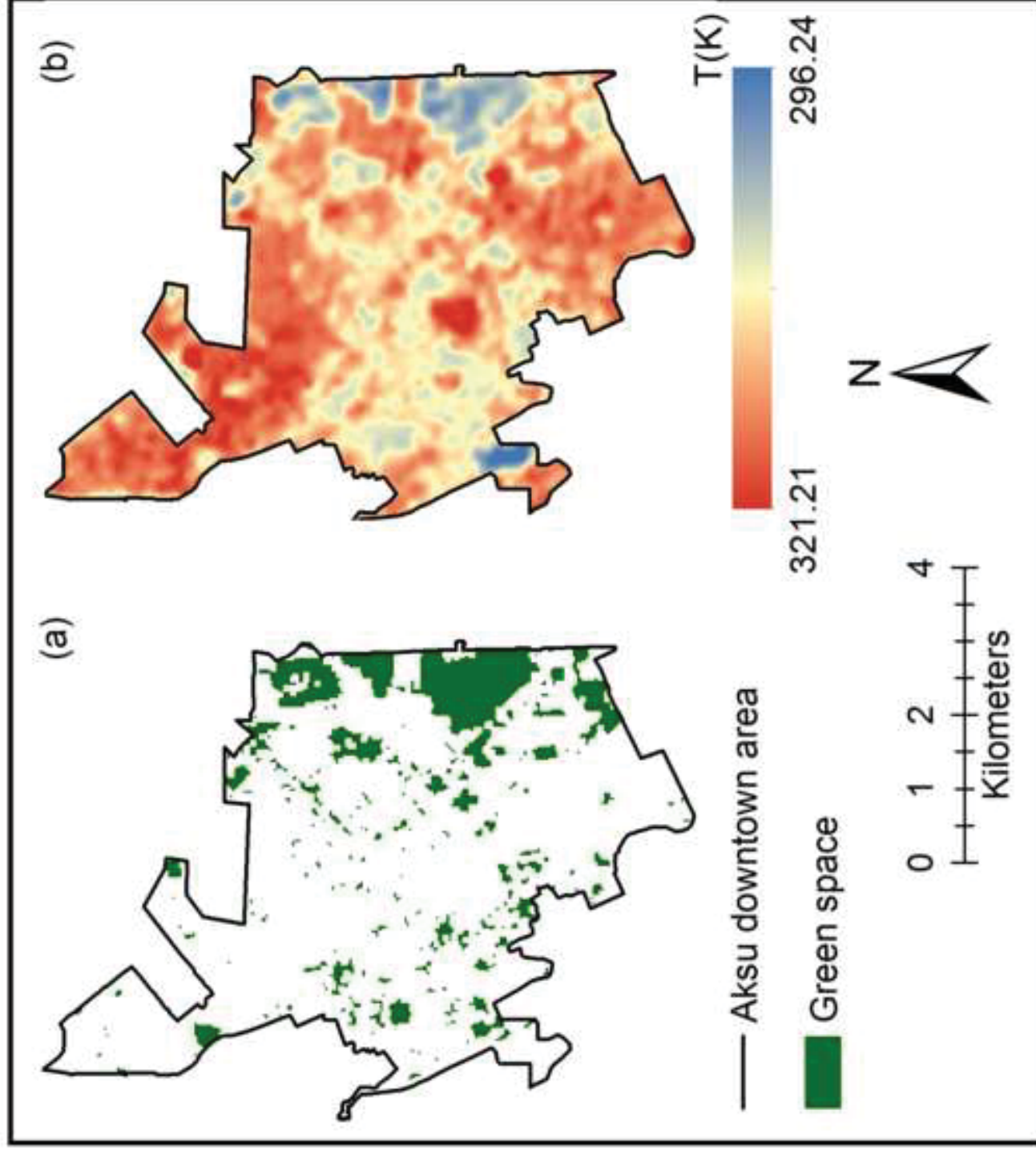




Figure 3  
[Click here to download high resolution image](#)

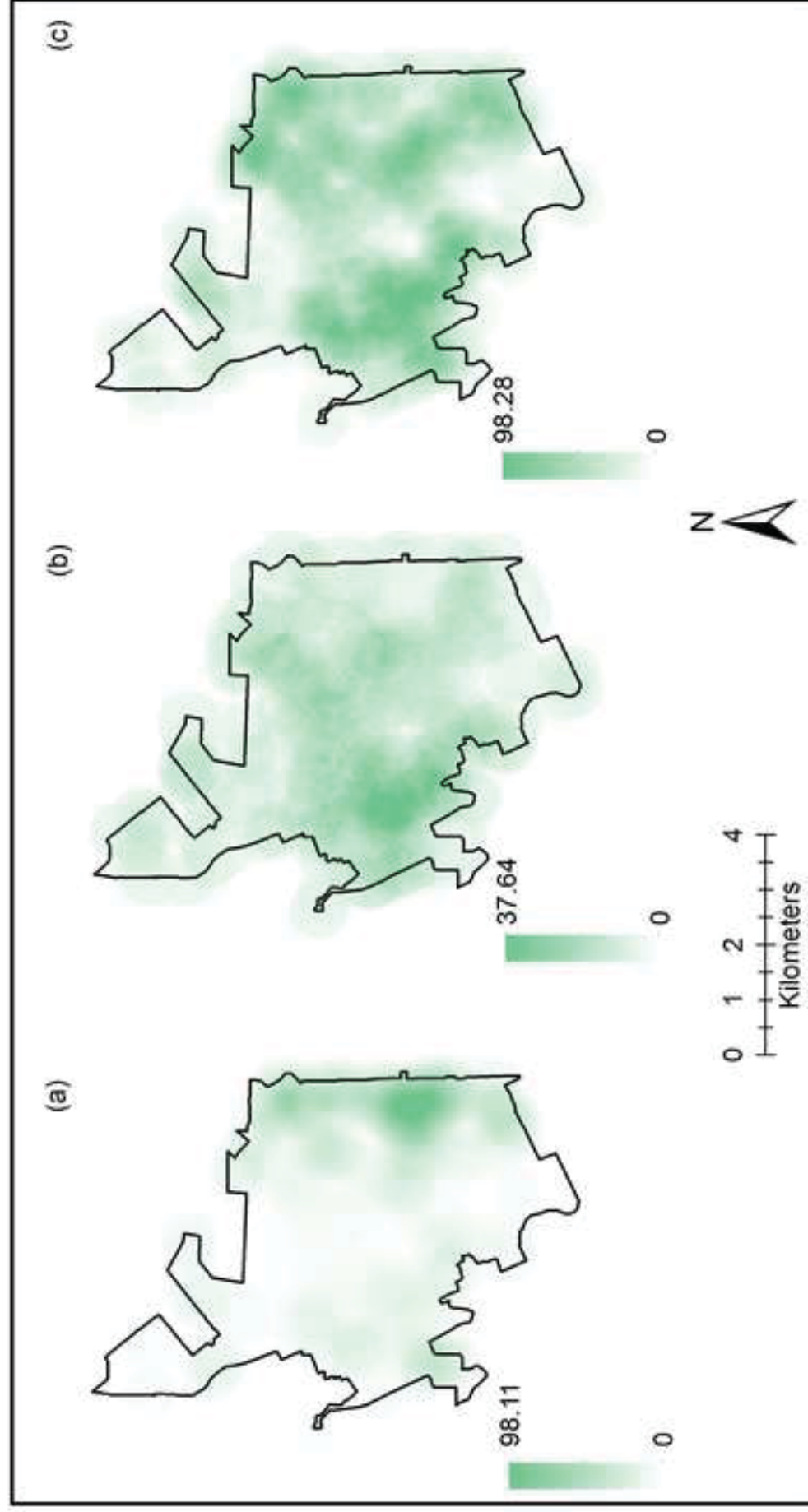
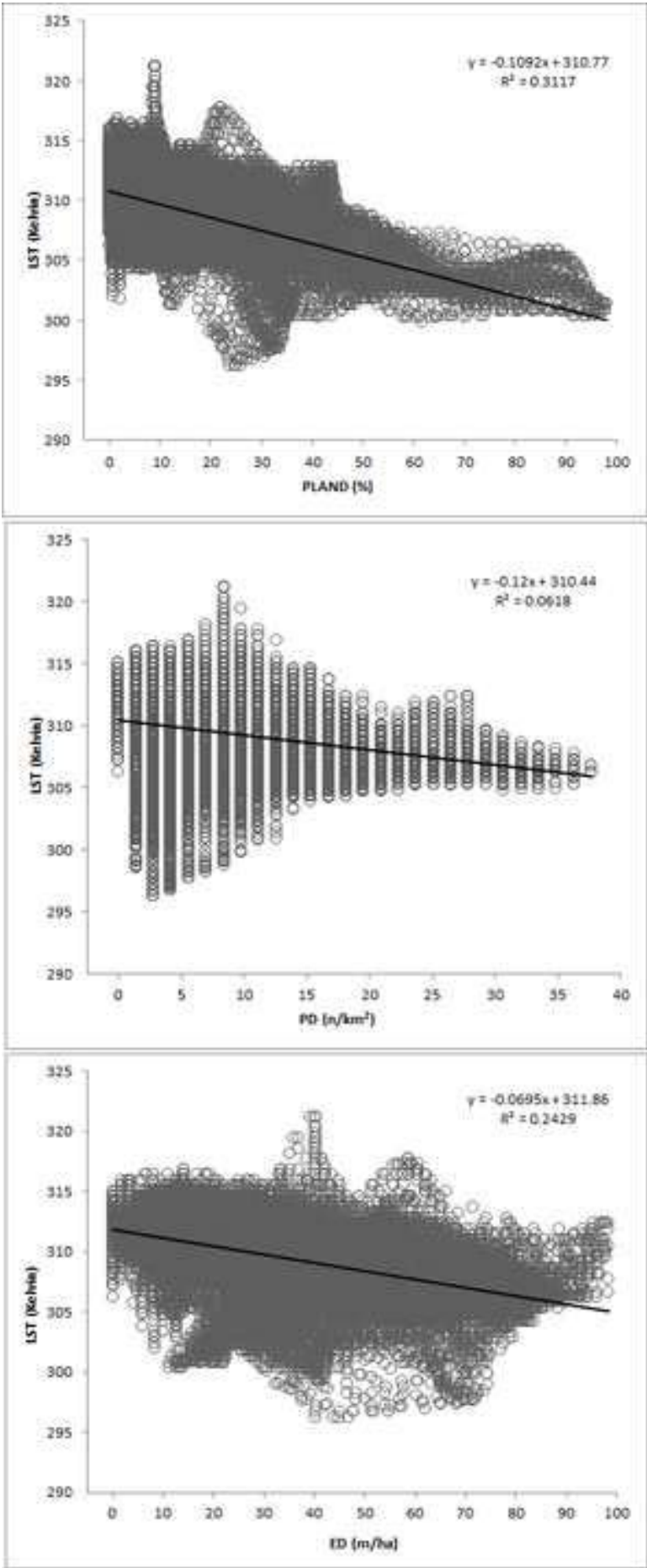


Figure 4  
[Click here to download high resolution image](#)



**Table 1**

[Click here to download Table: Table 1 Accuracy assessment of the urban green space derived map.docx](#)

Table 1 Accuracy assessment of the urban green space classification map.

	Reference data (Pixels)				Total	User's accuracy (%)
	Urban green space	Residential area	Construction site	Water body		
Urban green space	231	6	2	2	241	95.9
Residential area	0	170	15	2	187	90.9
Construction site	1	53	148	2	202	73.3
Water body	0	11	0	99	110	90.0
Total	232	240	165	103	740	
Producer's accuracy (%)	99.6	70.8	89.7	96.1		
Overall Accuracy (%)	87.6					
Kappa coefficient	0.83					

**Table 2** Landscape metrics used in this study(Mcgarigal et al., 2002)

Metrics (abbreviation)	Calculation and description
<i>Compositional</i>	
Percentage of Landscape (PLAND)	$100/A \times \sum_{i=1}^n a_i$ Proportional abundance of green space in the landscape (%)
<i>Configurational</i>	
Patch density(PD)	$n/A \times 10^6$ Number of green space patches divided by total landscape area (n/km <sup>2</sup> )
Edge density(ED)	$10,000/A \times \sum_{i=1}^n e_i$ Total length (border not included) of all edge segments of green space per hectare (m/ha)

---

$a_i$  area of patch  $i$ ;  $e_i$  length of edge (or perimeter) of patch  $i$ ;  $A$  landscape area;  $n$  number of patches

**Table 3**  
[Click here to download Table: Table 3 Normalized mutual information results of compositional configuration of green space and](#)

**Table 3** Normalized mutual information results of compositional configuration of green space and landscape metrics

$C_{XY}$		Normalized mutual information
$X$	$Y$	value
PLAND		0.7100
PD		0.6985
ED		0.7033
PLAND, PD	LST	0.7679
PLAND, ED		0.7650
PD, ED		0.7832
PLAND, PD,ED		0.8694